

DGRO: Diameter-Guided Ring Optimization for Integrated Research Infrastructure Membership

Shixun Wu[†], Krishnan Raghavan[‡], Sheng Di[‡], Zizhong Chen[†], Franck Cappello[‡]

[†]University of California, Riverside, CA, US

[‡]Argonne National Laboratory, Lemont, IL, US

swu264@ucr.edu, kraghavan@anl.gov, sdi1@anl.gov, chen@cs.ucr.edu, cappello@mcs.anl.gov

Abstract—Logical ring is a core component in membership protocol. However, the logic ring fails to consider the underlying physical latency, resulting in a high diameter. To address this issue, we introduce Diameter-Guided Ring Optimization (DGRO), which focuses on constructing rings with the smallest possible diameter, selecting the most effective ring configurations, and implementing these configurations in parallel. We first explore an integration of deep Q-learning and graph embedding to optimize the ring topology. We next propose a ring selection strategy that assesses the current topology’s average latency against a global benchmark, facilitating integration into modern peer-to-peer protocols and substantially reducing network diameter. To further enhance scalability, we propose a parallel strategy that distributes the topology construction process into separate partitions simultaneously. Our experiment shows that: 1) DGRO efficiently constructs a network topology that achieves up to a 60% reduction in diameter compared to the best results from an extensive search over 10^5 topologies, all within a significantly shorter computation time, 2) the ring selection of DGRO reduces the diameter of state-of-the-art methods Chord, RAPID, and Perigee by 10%-40%, 44%, and 60%. 3) the parallel construction can scale up to 32 partitions while maintaining the same diameter compared to the centralized version.

I. INTRODUCTION

Researchers increasingly require cross-platform utilization of diverse computing and storage devices [1, 2, 3, 4, 5]. The U.S. Department of Energy (DOE) recognizes the persistent trend of integrated research infrastructure (IRI) as the future of scientific computing [6]. These intricate science workflow processes utilize geographically dispersed computational resources across multiple facilities [7]. However, the diversity and distributed nature of these resources, managed by different organizations, domains, and communities, present significant challenges in fully leveraging their capabilities [8]. Consequently, effective membership management and reliable failure detection are crucial for the stability and efficiency of these systems.

Moreover, at such scales, system failures are commonplace rather than exceptions [9, 10]. Researchers encounter numerous issues, including application code errors [11], authentication issues, network disruptions [12], workflow system breakdowns [11], filesystem and storage complications [13], and hardware faults [14, 15, 16, 17, 18, 19]. Enhancing the computational platform’s performance and resilience making it fault-tolerant, robust against a variety of workloads and environmental conditions, and adaptable to changes in workloads, resource availability, and connectivity is crucial for enabling researchers to pursue their scientific goals efficiently and effectively [20].

Membership management solutions in modern systems can generally be categorized into two types, centralized or decentralized gossip-based. The first is a centralized strategy, such as Slurm [21], etcd [22], or Chubby [23], or ZooKeeper [24], to manage the membership list. This approach offers simplicity by maintaining a centralized list with strong consistency, which other processes periodically access. However, this centralization can limit system resilience, as failures or connectivity issues within this small cluster could compromise service availability [24, 25, 26]. The second category comprises gossip-based, fully decentralized methods [27, 28, 29, 30, 31, 32], which offer enhanced resilience by distributing the membership information across the network, thereby reducing reliance on a central point of failure. Gossip-based membership. van Renesse et al. [33, 34] was proposed to handle membership by utilizing gossip to disseminate positive notifications (keepalives) among all processes. If a process p crashes, other processes will eventually remove p after a timeout period. SWIM [35] introduced a variation of this method, which minimizes communication overhead by using gossip to distribute “negative” alerts instead of the usual positive notifications. Nowadays, gossip-based membership protocols are commonly implemented in various deployed systems, such as ScyllaDB [32], Akka [28], Redis Cluster [29], Cassandra [27], Orleans [30], Netflix’s Dynomite [25], Uber’s Ringpop [31], and systems at Twitter [36].

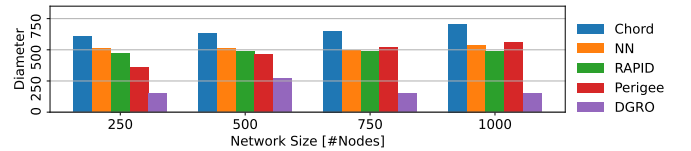


Figure 1: DGRO has low diameter.

Decentralized gossip protocols commonly utilize a logical ring, structured by consistent hashing, which is inherently random and disregards the physical network layout. This randomness often leads to inefficiencies, as the ring fails to minimize network diameter and thus exacerbates latency issues. As shown in Figure 1, state-of-the-art has a diameter up to 3 times higher than our DGRO.

In contrast, we address the inefficiencies of suboptimal ring topologies through our Diameter-Guided Ring Optimization (DGRO) approach, which tackles the problem from three key perspectives: 1) determining the minimum possible diameter for a given fixed degree, 2) selecting the most effective ring

topology based on a given latency distribution, and 3) exploring the feasibility of constructing ring topologies in parallel without compromising the overall diameter, thus aiming to reduce the time consumption associated with sequential builds.

We summarize our contributions as follows:

- We develop, DGRO, a diameter-guided ring optimization for integrated research infrastructure membership. DGRO is characterized by a ring optimization with a hybrid strategy of human heuristics and reinforcement learning, achieves a low diameter compared to other state-of-the-art methods.
- We design a Q-learning method with graph embedding to build a ring topology with low diameter. Q-learning is used to avoid local optima and greedy selection commonly found by human heuristics. This method selects nodes by utilizing a q-function to estimate future states rather than relying on a one-step greedy algorithm, minimizing the network diameter.
- DGRO dynamically selects an appropriate ring topology by comparing the average latency of the current topology against a range established by the global minimum and average latencies. This self-adaptive strategy can be integrated into contemporary peer-to-peer protocols, leading to a significant reduction in network diameter.
- We propose a parallel strategy to enhance the topology construction process, achieving the same diameter as the sequential build while speeding up by 32x.
- Experimental results show that: 1) DGRO efficiently constructs a network topology that achieves up to a 60% reduction in diameter compared to the best results from an extensive search over 10^5 topologies, all within a significantly shorter computation time, 2) the ring selection of DGRO reduces the diameter of state-of-the-art methods Chord, RAPID, and Perigee by 10%-40%, 44%, and 60%. 3) the parallel construction can scale up to 32 partitions while maintaining the same diameter compared to the centralized version.

The rest of this paper is arranged as follows: §II introduces background and related works. §III describe the system model and performance metrics for our research. §IV demonstrates the framework of DGRO. The design of self-adaptive ring selection is detailed in §V, and the design of parallel ring construction is proposed in §VI. In §VII, the evaluation results are presented and analyzed. Finally, §VIII concludes and discusses future work.

II. BACKGROUND AND RELATED WORK

A. Physical Diameter Matters

The diameter of a graph is the longest shortest path between any two vertices, representing a critical metric in network design, such as in information, social, and communication networks. It measures the maximum distance for direct communication within the network. A smaller diameter is vital for enhancing network efficiency by reducing latency in systems like multi-core processor networks [37] or by creating highly influential networks for campaigns in small-world network models [38].

Extensive research has focused on reducing the diameter of undirected graphs by adding new edges, a method commonly

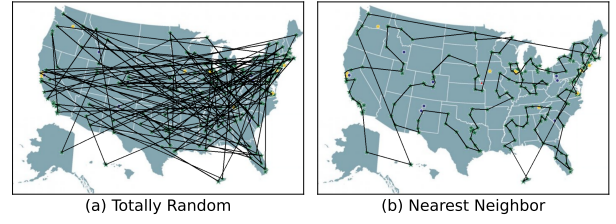


Figure 2: 117 research sites located within U.S. Both (a) random ring and (b) nearest neighbor ring may introduce inefficient long jump between two geologically close nodes.

referred to as “shortcutting” in scholarly literature [39, 40, 41, 42]. These added edges are known as shortcut edges. A specific challenge in this area, the Bounded Cardinality Minimum Diameter (BCMD) problem, was formulated by Li, McCormick, and Simchi-Levi [43]. The objective in BCMD is to add a limited number of shortcut edges, typically no more than k , to reduce the overall diameter of the graph efficiently.

A notable limitation of the Bounded Cardinality Minimum Diameter (BCMD) problem is that optimal solutions, or their approximations, may significantly increase the degree of a single vertex. This increase is a typical outcome from prevalent approximation algorithms for BCMD, which often involve dividing the graph into $k+1$ distinct clusters and then connecting these clusters through a method called star-shortcutting. This process involves selecting a central vertex from one cluster and connecting it to the centers of all other clusters, consequently adding up to k shortcut edges and increasing the degree of the central vertex by k . However, for many practical applications, it is important to limit the degree increase of any single vertex due to physical, economic, or other practical constraints. These constraints are commonly found in various real-world network challenges [41, 44]. For instance, Bokhari and Raza [45] explored methods to decrease the diameter of computer networks by adding additional connections while ensuring that no more than one I/O port is added to each processor. Another scenario is in social networks, where service providers may want to suggest new friendships to enhance network connectivity and facilitate information spread while reducing polarization [46, 47, 48]. In such cases, as noted in [48], the largest distance between members of different groups—termed the colored diameter—serves as a polarization metric. A more prudent approach might involve restricting the number of new connections recommended to each user to prevent overwhelming them and to ensure the practical materialization of these recommended links.

In contrast to the above methods, we focus on the construction of one or multiple ring topologies that achieve a low diameter under degree constraints. In Figure 2, both the random and nearest neighbor include long paths even between adjacent nodes.

B. Graph Embedding & Deep Q-learning

The recent advancements in using deep learning architectures for solving combinatorial problems, such as the Traveling Salesman Problem (TSP) [49, 50, 51, 52, 53, 54, 55], highlight the potential of the combination of reinforcement learning and

graph embedding. These techniques are particularly effective in addressing the inherent complexities of combinatorial optimization. While existing architectures have struggled with efficiently capturing the combinatorial structure of graph problems and required extensive training data [50], reinforcement learning and graph embedding can provide more tailored and efficient solutions.

Moreover, the TSP shares similarities with ring optimization tasks, where the objective is to construct optimal loops, akin to finding the shortest possible route that visits each city once in TSP. Although both involve the construction of cycles, the primary difference lies in the objective or reward function used to evaluate solutions. In TSP, the goal is to minimize the total traveling distance, whereas ring optimization is to minimize the overall diameter. By adapting the methodologies developed for TSP, using reinforcement learning and graph embeddings, one can potentially find a better topology in terms of diameter.

III. SYSTEM MODEL

A. Network Model

We model the integrated research infrastructure (IRI) peer-to-peer (P2P) network as an undirected graph $G(V, E)$, where V represents the set of nodes and E denotes the set of edges, or links, between these nodes. A node corresponds to master machines (e.g., SLURM controller daemons) that can accept inter-cluster TCP connection requests from other servers and compute nodes. In contrast, compute nodes in the IRI are dedicated computing devices that cannot accept external TCP connection requests. Once a TCP connection is established between two nodes, communication flows bidirectionally.

In this work, we focus on the controller nodes, which form the core of the P2P overlay network. These nodes are typically always active, and the latency of membership changes is highly influenced by the interconnection network between them. Our objective is to minimize inter-cluster synchronization latency, not data transmission latency, a goal that is formally defined in §2.2. Our proposed topology optimization approach is generalizable and can be adapted to improve synchronization times for compute nodes as well.

For any pair of nodes (u, v) in the set V , the latency $\delta(u, v)$ for sending a message between them via a TCP connection is assumed to be a constant non-negative value. This latency encompasses all transmission delays including in-network factors such as propagation and queuing. The value of $\delta(u, v)$ is influenced by several variables, including the size of the transmitted messages, the internet access bandwidth available at nodes u and v , the physical distance between these nodes, and the level of network congestion. These factors are considered to be slowly varying relative to the timescale of our algorithm. Additionally, each node v in V incurs a fixed processing time Δ_v for handling membership update messages, which varies based on the computing performance of the node.

We posit that membership status is periodically broadcast across the network. When a node u either initiates a membership message or receives one from an incoming neighbor, it promptly relays this message to each of its outgoing neighbors. The

completion of this relay for each neighbor v occurs within a designated time $\delta(u, v)$. This model assumes that the broadcast mechanism is immediate and sequential, ensuring rapid dissemination of membership updates throughout the network.

At any given time, each node in the network maintains $\log(N)$ outgoing connections (d_{out}) and an equivalent number of incoming connections (d_{in}). To maintain the membership protocol, each node also keeps a local database, which is routinely updated through message exchanges with neighboring nodes. Newly joined peers acquire the membership list from existing nodes. We assume that each node is aware of the IP addresses of all other nodes in the network.

B. Performance Metrics

Given a fully connected P2P network, our objective is to construct one or multiple rings to minimize the diameter. The degree-constrained minimum diameter problem is an NP-hard problem [56].

IV. DGRO: OPTIMIZE RING TOPOLOGY OVER GRAPHS

A. Degree Constrained Subgraph with Minimum Diameter

Given a weighted complete graph $G = (V, E)$ where V is the set of vertices and E is the set of edges with associated weights $w : E \rightarrow \mathbb{R}^+$, the problem is to find a subgraph $G' = (V, E')$, where: V is the set of all vertices from G , $E' \subseteq E$, and each vertex $v \in V$ has degree not exceeds K in G' . The objective is to minimize the diameter $D(G')$ of the subgraph G' . The diameter is defined as:

$$D(G') = \max_{u, v \in V} d(u, v), \quad (1)$$

where $d(u, v)$ representing the shortest path distance between vertices u and v in G' , considering the weights of the edges. This problem seeks to optimize the connectivity and compactness of G' by minimizing its diameter while maintaining the degree constraint K for each vertex.

B. Ring Construction

A solution is constructed by sequentially adding edges into a partial solution [56].

- **Input:** a complete graph $G = (V, E)$, initial subgraph $G_0 = (V, E_0)$, weights matrix W and degree constraint K , where $|V| = N$, $W \in \mathbb{R}^{N \times N}$, $K \in \mathbb{Z}^+$.
- **Sequential Addition:** Add an edge e_t to the partial solution G_t

$$G_t = (V, E_t) \xrightarrow{e_t} G_{t+1} = (V, E_t \cup \{e_t\}),$$

and the degree constraint, $\text{degree}(v) \leq K, \forall v \in V$, is satisfied.

- **Selection Strategy:** Select the edge with the highest score based on a scoring function $F(G, G_t)$.

$$e_t = \arg \max_{e \in E \setminus E_t} F(G, G_t, e).$$

The *nearest-neighbour heuristic* adopts the edge weight $w(e)$ as the score function, namely $F(G, G_t, e) = w(e)$.

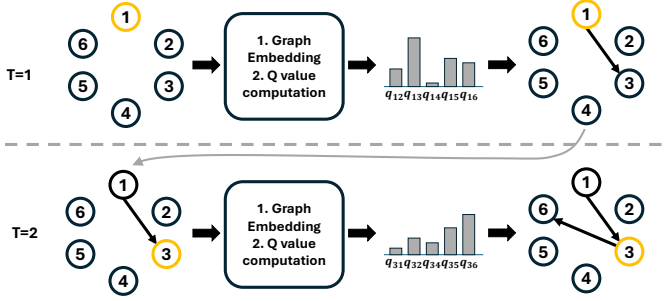


Figure 3: Node selection with DGRO

- **Termination:** $|E_t| \geq K \cdot N$ or all left edges $e \in E \setminus E_t$ cannot satisfy the degree constraint¹.

Defining a scoring function is an implicit task without a straightforward functional expression. Using the edge weight as the scoring function is a useful heuristic, but it is not exactly aligned with the goal of minimum diameter. In contrast, a neural network can develop a more effective scoring function than human-designed heuristics. By training on rewards derived from sampling, the neural network can generate scores that better reflect the impact of a selection on future graph construction and the diameter. We next formulate the diameter optimization problem with Markov Decision Process (MDP).

C. Markov Decision Process Formulation

In the formulation discussed last section, e_t is chosen from $E \setminus E_t$, requires scoring $K \cdot N$ to N^2 edges, depend on $|E_t|$. To reduce complexity, we select e_t from $\{(v_t, u) | u \in V\} \setminus E_t$, where v_t is the end node of last chosen edge $e_{t-1} = (v_{t-1}, v_t)$. Hence, the state becomes $S_t = (W, W_t, v_t)$ and the score function is

$$F(G, G_t, e_t) = Q(S_t, u; \Theta).$$

$Q(S_t, u; \Theta)$ is a neural network takes S_t as input and output a score of edge (v_t, u) , where Θ is the network weights. The action space is defined as $[1, \dots, N]$, where N represents the number of nodes within the graph. The state is characterized by the latency matrix in conjunction with the topology that has been constructed up to the current step.

The reward function is computed as the difference in diameters between consecutive states, specifically, $r(S_t, S_{t+1}) = D(G_t) - D(G_{t+1}) - \alpha w(a_t, a_{t+1})$, where D is the diameter, S_t and S_{t+1} (a_t and a_{t+1}) represent the state (action) at time t and $t + 1$, respectively. With this reward function, the diameter term of cumulative reward will be

$$\sum_{t=0}^{T-1} D(G_{t-1}) - D(G_t) = D(G_0) - D(G_T).$$

Because we start from an empty topology, $D(G_0)$ is set to a constant. Hence, the cumulative reward of an episode will become the diameter of the final topology, namely $D(G_T)$, which is exactly our optimization objective. When the graph

¹e.g. for $N = 20, K = 4$, the front 19 nodes consist a graph with degree 4, while the node 20 still has degree 2 and no more edges can be connected between node 20 to any nodes from 1 – 19.

G_t is not connected, the diameter of the largest connected component is adopted. Besides, we augment the reward function with an additional term $\alpha w(a_t, a_{t+1})$ to mitigate the incidence of zero rewards because the diameter tends to stabilize and becomes difficult to reduce further once more than half of the edges have been added to the topology. $w(a_t, a_{t+1})$ represents the latency of the connection between nodes a_t and a_{t+1} , and α is a coefficient controlling the weight of the latency term. This modification to the reward function is intended to incentivize actions that not only improve the diameter but also consider the latency of individual connections, thus enhancing the overall network performance.

Algorithm 1 Diameter-Guided Ring Construction.

input: start node v_0 , Q-network $Q(\cdot; \Theta)$, latency matrix A
output: optimized ring ($v_0 \rightarrow \dots \rightarrow v_{N-1} \rightarrow v_0$).
for step $t = 1$ to T **do**
 $v_t = \arg \max_v \hat{Q}(S_t, v; \Theta)$
Add v_t to partial solution: $S_{t+1} := (S_t, v_t)$
end for

Algorithm 1 demonstrates the ring construction with Q value as a score function. In Figure 3, we provide a specific example of our method in action. Starting from node 1, our algorithm calculates the Q-values $q_{12}, q_{13}, \dots, q_{16}$ for connections from node 1 to nodes 2 through 6. The algorithm selects the node associated with the highest Q-value among these, which in this example is node 3 due to q_{13} being the largest. Consequently, the action taken in this step is to establish a connection from node 1 to node 3. In the subsequent step, the algorithm recalculates the Q-values for connections from node 3 to the remaining nodes and selects the next action in a similar manner, continuously optimizing the network structure based on these Q-value assessments. This sequential decision-making process effectively builds the network topology by linking nodes that maximize the predicted Q-value, thereby optimizing the overall connectivity based on the learned Q-function.

D. Graph Embedding

Due to the substantial memory demands and learning inefficiencies of using the adjacency matrix as a direct input, which would require at least N^2 network parameters, we’ve opted for a graph embedding approach. This method encodes the neighborhood and latency information of each node into a one-dimensional vector with a feature dimension p . This embedding technique effectively reduces the complexity and enhances the scalability of our model, making it more feasible for handling large networks without a significant loss in performance or detail.

Eqn. (2) is the embedding strategy for the complete graph G and the partial solution subgraph G_t . In Eqn. (2), $\mu_v^{(t)} \in \mathbb{R}^p$ is the embedding vector of node v after t iteration, the initial embedding is a zero vector, x_v is the degree of node v , $\mathcal{N}(v)$ is the neighbour of node v , $\theta_1 \in \mathbb{R}, \theta_2, \theta_3 \in \mathbb{R}^{p \times p}, \theta_4 \in \mathbb{R}^p$. By applying Eqn. (2) for T iterations, we get the final embedding vector $\mu_v^{(T)}$. After we get the node embedding $\mu_v^{(T)}$, we combine

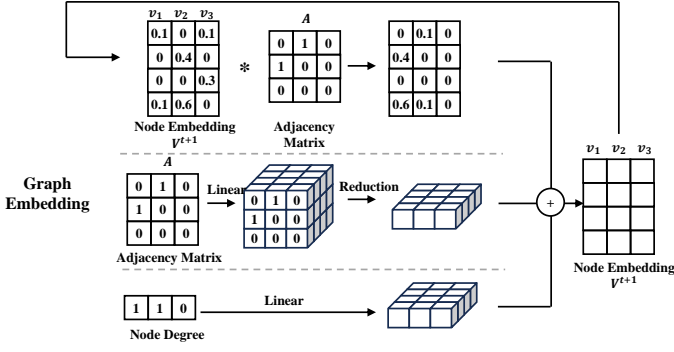


Figure 4: Graph Embedding

the embeddings of all nodes sum, source node v_{t+1} , target node u and the weight $w(v_{t+1}, u)$ into $x \in \mathbb{R}^{3p+1}$, as shown in Eqn. (3). Finally, x is forwarded to a MLP to get the final score of selection edge $e_{t+1} = (v_t, u)$.

$$\mu_v^{(t+1)} \leftarrow \text{relu} \left(\theta_1 x_v + \theta_2 \sum_{u \in \mathcal{N}(v)} \mu_u^{(t)} + \theta_3 \sum_{u \in \mathcal{N}(v)} \text{relu}(\theta_4 w(v, u)) \right) \quad (2)$$

$$x \leftarrow [w(v_t, u), \theta_5 \sum_{v \in V} \mu_u^{(T)}, \theta_6 \mu_{v_t}^{(T)}, \theta_7 \mu_u^{(T)}] \quad (3)$$

$$\hat{Q}(S_t, u; \Theta) = \theta_{10}^\top \text{relu}(\theta_9 \text{relu}(\theta_8 \text{relu}(x))) \quad (4)$$

Figure 4 illustrates how we optimize performance by transforming embeddings into matrix multiplication operations. The first row depicts the multiplication of node embeddings with the latency matrix, which corresponds to the term $\theta_2 \sum_{u \in \mathcal{N}(v)} \mu_u^{(t)}$ in Equation 2. The second row processes the latency matrix through a linear layer first, then performs a weighted reduction along the column direction based on the weights of the latency matrix, aligning with the term $\theta_3 \sum_{u \in \mathcal{N}(v)} \text{relu}(\theta_4 w(v, u))$.

E. Learning Algorithm

Standard 1-step Q-learning updates the parameters of the function approximator at each step within an episode by performing a gradient descent step aimed at minimizing the squared loss.

$$\left(y - \hat{Q}(S_t, v_t; \Theta) \right)^2, \quad (5)$$

where $y = r(S_t, S_{t+1}) + \gamma \cdot \hat{Q}(S_{t+1}, v_{t+1}; \Theta)$.

Algorithm 2 illustrates the training framework with an experience replay mechanism. Initially, a memory buffer is established to store transitions, aiding in the machine-learning process across multiple epochs. Each epoch involves sampling a graph and constructing a solution iteratively, where node selections are based either on randomness (to explore diverse paths) or on maximizing expected rewards via a Q-value function (to exploit known strategies). Critical to this approach is the dynamic updating of the solution state with each new node addition, influenced by prior actions stored in the replay

memory. These experiences are randomly revisited to update the learning model's parameters through stochastic gradient descent, ensuring continual refinement of the strategy. The process iteratively enhances the model's ability to predict and execute optimal actions, culminating in a robust set of parameters that define the most effective decision-making process for the types of graphs encountered.

Algorithm 2 Q-learning for DGRO

Initialize experience replay memory \mathcal{M} to capacity N

for epoch $e = 1$ to L **do**

Draw graph G from distribution \mathcal{D}

Initialize the state to empty $S_1 = ()$

for step $t = 1$ to T **do**

$v_t = \begin{cases} \text{random node } v \in S_t, & \text{with probability } \epsilon \\ \arg \max_v \hat{Q}(S_t, v; \Theta), & \text{otherwise} \end{cases}$

Add v_t to partial solution: $S_{t+1} := (S_t, v_t)$

if $t \geq n$ **then**

Add tuple $(S_{t-1}, v_{t-1}, R_{t-1,t}, S_t)$ to \mathcal{M}

end if

Sample random batch from $B \sim \mathcal{M}$

Update Θ by SGD over B

end for

end for

return Θ

V. SELF ADAPTIVE RING TOPOLOGY OPTIMIZATIONS

In subsequent experiments, deep Q-learning proved capable of outperforming heuristic-based solutions for networks with up to 200 nodes. However, as the number of nodes increases, the computational power and training time required also increase significantly, limiting the scalability of Q-learning. This is particularly evident in K-ring topologies, where the number of required steps scales with $K \times N$, and K typically takes a value of $\log_2(N)$. For instance, with $N = 500$, around 4500 steps are necessary. Given these constraints, simple rule-based heuristic algorithms remain essential under such conditions.

Our findings indicate that the choice of ring based on different heuristics significantly impacts the total diameter of peer-to-peer (P2P) topologies. Therefore, we have designed a decentralized scheme that allows the P2P network to automatically adjust its ring topology based on the current latency conditions, enhancing network performance dynamically. This approach facilitates more efficient network configurations that adapt in real-time to changing operational environments.

Algorithm 3 assesses network topology based on latency characteristics. In Algorithm 3, each node randomly samples K nodes from both its existing connections and the entire network to test latencies, denoted as L_{local} and L_{global} , respectively. The algorithm proceeds to calculate the average values of both L_{local} and L_{global} , as well as the minimum value within L_{global} . Using a gossip protocol, these three values from all nodes are then aggregated and averaged. The process concludes by summing up and outputting these aggregated measurements, effectively providing a comprehensive view of the network's latency

Algorithm 3 Gossip-based Latency Measurement

```

1: Input: network  $G = (V, E)$ , time period  $T$ , #samples  $K$ .
2: Output:  $\bar{L}_{local}, \bar{L}_{global}, \bar{L}_{min}$ 
3: Initialize  $L_{local} \leftarrow 0, L_{global} \leftarrow 0, L_{min} \leftarrow 0$ 
4: for each node  $u \in G$  do
5:   Randomly select  $\{r_i\}_{i=1}^K$ , s.t.  $(u, v_i) \in E$ .
6:   Randomly select  $\{v_i\}_{i=1}^K$ .
7:    $L_{local} = \frac{1}{K} \sum_{i=1}^K L(u, r_i)$ 
8:    $L_{global} \leftarrow \frac{1}{K} \sum_{i=1}^K L(u, v_i)$ 
9:    $L_{min} \leftarrow \min_{i=1}^K L(u, v_i)$ 
10: end for
11: Initialize zero to  $L_{local}, L_{global}, L_{min}, M$ 
12: for each node  $u \in G$  do
13:   for each round do
14:     Gossip ( $L_{local}, L_{global}, L_{min}$ ) to neighbors
15:     Accumulate received  $L_{local}, L_{global}$ , and  $L_{min}$ 
16:     Update message count  $M \leftarrow M + 1$ 
17:   end for
18:   Wait for  $T$  for convergence
19: end for
20: Compute averages:
21:  $\bar{L}_{local} \leftarrow \sum L_{local} / M$ 
22:  $\bar{L}_{global} \leftarrow \sum L_{global} / M$ 
23:  $\bar{L}_{min} \leftarrow \sum L_{min} / M$ 
24: return  $\bar{L}_{local}, \bar{L}_{global}, \bar{L}_{min}$ 

```

landscape. This method allows for a decentralized assessment of network performance, facilitating optimal adjustments to the network configuration based on real-time latency data.

Once the period T has elapsed, each node calculates the ratio $\rho = \frac{L_{local} - L_{min}}{L_{avg} - L_{min}}$ to assess whether the current topology is either too concentrated or too random. This metric provides a standardized measure of network structure by comparing the dispersion of local latencies relative to the minimal and average latencies observed across the network. A value close to 0 or 1 indicates a topology that is either too clustered or excessively dispersed, respectively, suggesting potential inefficiencies in data routing and network resilience. This evaluation helps in identifying areas where the network topology may need adjustments to optimize performance and reliability.

To manage the network topology efficiently based on latency distribution, we can set a threshold ϵ . If the calculated ratio $\rho > \epsilon$, it indicates that the distribution is too clustered. Then an additional pre-designed random ring can be introduced to diversify node connections and decrease network clustering. Conversely, if the distribution appears too sparse, with $\rho > 1 - \epsilon$, incorporating the shortest ring can help tighten the network's topology by connecting nodes that are closer together in terms of latency. This adaptive approach allows for dynamic adjustments to the network's structure, optimizing performance based on real-time analysis of latency characteristics. The shortest ring is constructed by sequentially selecting the nearest available neighbor.

A. Impact of different ring topology on p2p overlays

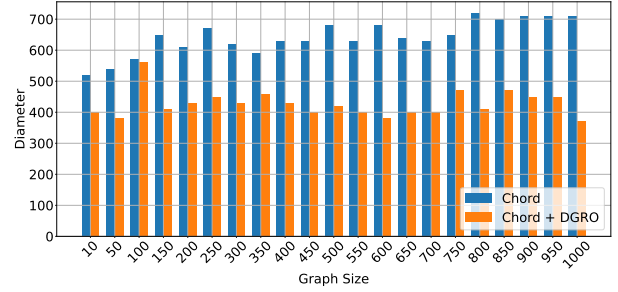


Figure 5: DGRO helps Chord reduce diameters.

1) *Chord*: Chord [57] assigns each node and data item a unique identifier, allowing nodes to locate resources within a logarithmic number of steps relative to the total number of nodes in the network. The unique identifier is given by a hashing function, which forms a logical ring among all nodes. Due to the randomness of the logical ring, Chord shows a ρ close to 1. By replacing the random ring with the shortest ring, the diameter is reduced by 10% to 40%, as shown in Figure 5.

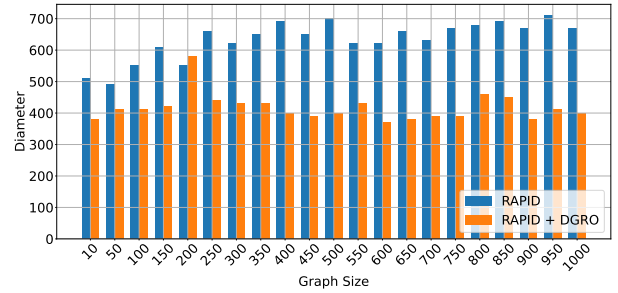


Figure 6: DGRO helps RAPID reduce diameters.

2) *RAPID*: Although the K-Ring topology [31] is a good expander, the system model does not consider the latency between each node. The consistency hash function used to generate the K-Ring topology is fully randomized, which results in a high diameter, as shown in Figure 7. By switching one of the random rings to the shortest ring, the diameter get a significant decrement up to 43%.

3) *Perigee*: Perigee [58] is a nearest-neighbor-based method and typically does not require a specific ring. Each node organizes its neighbors based on the timestamp of receiving a random global broadcast sourced from a neighboring node. Figure 7 compares the diameter of Perigee after adding a random ring and the shortest ring. Random ring has a low diameter compared to the shortest ring. For a high network size close to 1000, the improvement in diameter is up to 200%.

VI. PARALLEL

In addition to our existing strategies, we also experimented with a parallel construction approach for forming rings to decrease the number of sequential steps required in ring construction. This method is aimed at enhancing scalability by distributing the workload across multiple nodes simultaneously,

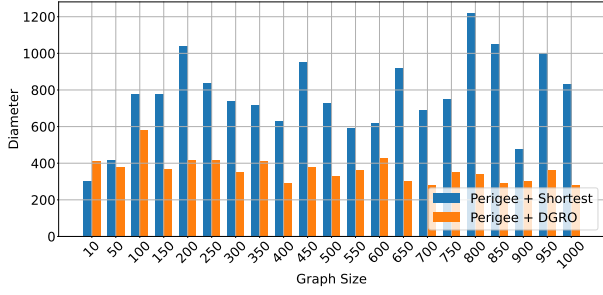


Figure 7: DGRO finds better diameters for Perigee.

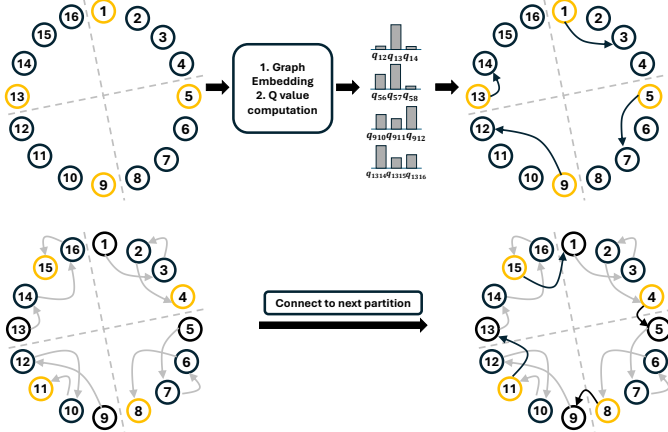


Figure 8: Parallel Ring Construction Workflow

thus significantly speeding up the overall process of ring formation.

This method involves dividing the N nodes into M partitions, thereby transforming a process that would typically require N sequential steps into a parallel procedure across M partitions. Each partition concurrently executes $\frac{N}{M}$ sequential steps internally. This approach effectively reduces the total time required for ring construction by parallelizing the work, thus enhancing scalability and efficiency in handling larger datasets or networks.

Algorithm 4 initiates by setting up a structure to accommodate the entire ring and then splits the total nodes N into M partitions, with each partition comprising roughly N/M nodes. In the parallel execution phase, each partition P_i independently constructs its segment of the ring. This is done by sequentially connecting nodes within the partition until all are linked, effectively closing the loop with the last node connecting back to the first in each partition. Once all partitions have completed their individual segments, these are merged into the main ring structure. To ensure the inclusivity of all nodes, especially when N is not perfectly divisible by M , the remaining nodes are added sequentially to complete the ring.

VII. PERFORMANCE EVALUATION

We evaluate the performance of DGRO, and compare it against the baseline algorithms of §V. Our experiments are based on a Python simulator we built following the network model of §III. We describe the experimental setting in §VII-A. Following this, we evaluate Perigee on a variety of different network

Algorithm 4 Parallel Ring Construction

- 1: **Input:** Total nodes N , Number of partitions M
- 2: **Output:** Constructed ring across partitions
- 3: Initialize an empty structure for the ring
- 4: Calculate partition size: $partition_size = N/M$
- 5: Divide nodes into M partitions
- 6: **for** each partition P_i in parallel **do**
- 7: Initialize local ring for P_i
- 8: **for** step = 1 to $partition_size$ **do**
- 9: Select the next node in P_i
- 10: Add node to the local ring of P_i
- 11: **if** step < $partition_size$ **then**
- 12: Node selection with DGRO
- 13: **else**
- 14: Connect last node in P_i to first node in P_{i+1}
- 15: **end if**
- 16: **end for**
- 17: Merge local ring of P_i into the main ring structure
- 18: **end for**
- 19: If there are any nodes left (due to integer division), add them sequentially to the main ring
- 20: **return** the main ring

conditions (§VII-C–§VII-D). All the mentioned *shortest rings* represent rings constructed by nearest neighbors.

A. Experimental Settings

1) *Network settings:* In our experiments, we evaluated the DGRO protocol using four distinct latency distributions to understand its performance under various network conditions. We used two synthetic distributions: a uniform distribution randomly sampled from the set $\{1, 2, \dots, 10\}$, namely $X \sim \text{Uniform}(1, 10)$ and a Gaussian distribution with a mean of 5 and a standard deviation of 1: $Y \sim \mathcal{N}(5, 1^2)$. Additionally, we incorporated two realistic latency distributions, FABIRC and Bitnode. FABIRC is based on latency data collected from 17 physical sites, which include 14 sites across the US, one in Japan, and two in Europe. Bitnode utilized latency of 1000 nodes. The nodes are randomly sampled from a list of 9,408 nodes. These nodes are distributed across seven geographic regions: North America, South America, Europe, Asia, Africa, China, and Oceania. For our experiment, the network size, link propagation, processing, and transmission delays were set as follows: (1) *Propagation Delay:* For FABIRC, we used the average one-hour measurement of one-way latency between each node pair. The propagation latency between a node u at site i and a node v at site j is calculated as $\text{latency}(i, j) + \text{latency}(u) + \text{latency}(v)$. The $\text{latency}(i, j)$ is measured from the FABIRC monitoring tool. For Bitnode, propagation latency was determined by geographical locations using the iPlane latency measurement dataset [58]. (2) *Message Size:* We assumed messages were small relative to the available bandwidth at the nodes, making the link propagation delays the dominant factor in message broadcasting delay. (3) *Message Processing Time:* Each node was assigned a mean message processing time of 1 ms. Additionally, each node

was configured to create and accept connections logarithmic to the network size, specifically $\log(N)$ outgoing and up to $\log(N)$ incoming connections. This experimental setup allowed us to explore the effects of network scalability in sections §5.2 and §5.3, varying network sizes to assess performance under different conditions.

2) *Algorithm compared:* We employed the topologies in CHORD, RAPID, and a nearest neighbor topology based on Perigee as compared baseline algorithm. Additionally, to establish a benchmark for the lowest possible network diameter, we utilized a genetic algorithm. For each graph instance, the genetic algorithm will search 100,000 topologies.

3) *Performance Metrics:* To evaluate the effectiveness of each network topology, we calculate the network diameter using the NetworkX library. We conducted our tests across various network sizes, specifically [50, 100, 150, ..., 1000]. For the FABRIC network, we selected 17 sites, assuming each site generates a varying number of nodes ranging from 1 to 58, resulting in total node counts from 17 to 986. The individual latencies $\text{latency}(u)$ and $\text{latency}(v)$ are assumed to follow a normal distribution with a mean of 5 and a standard deviation of 1, reflecting variability in node response times within each site. This setup allows us to model and analyze the impact of both inter-site and intra-site latencies on the overall network performance. For each network size, we performed 10 independent runs, each with randomly sampled link latencies. The results, showcasing the diameter for each network size, were plotted to provide a visual representation of performance across different scales. This methodological approach allows for a thorough analysis of how each topology performs under varying conditions and network sizes.

B. Optimize Ring with Deep Q-learning

We compare DGRO with Genetic Algorithm and random solution. The result of the genetic algorithm is searched over 100,000 graphs.

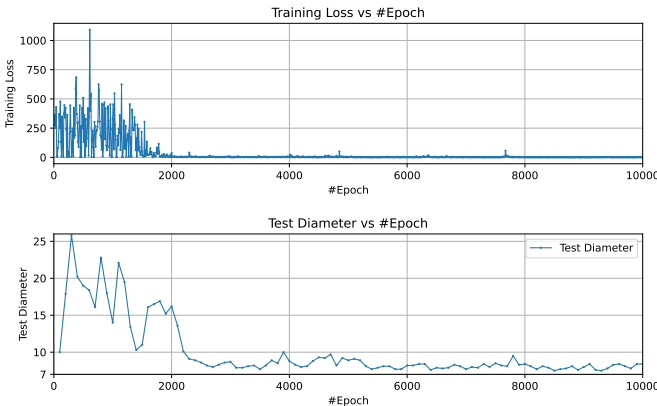


Figure 9: Training and Test Curve of DGRO.

1) *Hyperparameter and training settings:* We configured the graph embedding with a feature dimension $d = 16$ and a learning rate $\alpha = 5 \times 10^{-4}$. During training, we implemented an epsilon-greedy strategy where ϵ is dynamically adjusted with the formula $\epsilon = \max(1 - \frac{\text{epoch}}{2000}, 0.05)$. The replay buffer was set

to a length of 10^6 . We trained the model over 10^4 epochs with a batch size of 32. Each episode generates a new $N \times N$ matrix, with each element uniformly and randomly selected from the set $[1, 2, \dots, 10]$. Test graphs were generated using the same random sampling method.

As illustrated in Figure 9, the training curve converges after 2,000 epochs, while the test curve stabilizes at a diameter of 10 after 3,000 epochs. This demonstrates the efficacy of the training process over extended periods, highlighting the model's ability to consistently achieve optimal network topology as training progresses.

2) *Performance Evaluation:* We compare the diameter of the topologies constructed by DGRO with those generated by a genetic algorithm (GA) and a completely random ring. Figure 10 demonstrates the diameter while Figure 10 compares the inference time. Each method constructs a topology consisting of K rings, where each ring connects all nodes of the graph. For each graph instance, DGRO generates 10 different K -ring topologies. The 10 topologies are constructed with 10 different starting nodes. Then we select the one with the best diameter. In contrast, the GA searches through 1×10^5 different K -ring topologies to retain the one with the optimal diameter. For normalization, all calculated diameters are divided by the diameter of a random K -ring. This approach provides a clear comparison of the efficiency of DGRO against other methods in minimizing the network diameter across multiple configurations.

As shown in Figure 10 (a), DGRO outperforms the results of a brute force approach that iterates 100,000 times, and it does so with considerably lower inference time. As the network size increases, the effectiveness of the genetic algorithm degrades to the random method due to the exponential growth in combinatorial possibilities. Meanwhile, DGRO consistently reduces the random diameter to 40% of its original value. Figure 10 (b) shows DGRO has good scalability when problem size increases.

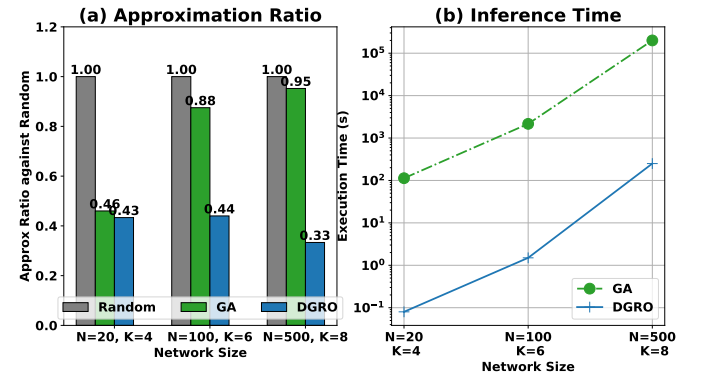


Figure 10: DGRO vs. Genetic Algorithm. The diameter is normalized by the result of a random ring.

C. Synthetic Latency

1) *Single heuristic ring:* The choice between different rings is primarily dependent on the network's overall diameter when focusing specifically on this metric. Employing a single heuristic, such as minimizing path length through the shortest ring or

random ring topology, may not always result in the most efficient outcomes in terms of diameter. Figure 11 illustrates the DGRO helps reduce the network diameters of CHORD, PERIGEE, and RAPID, under two different latency distributions: uniform and Gaussian. In both uniform and Gaussian latency distributions, DGRO helps RAPID and Chord switch to a shortest ring from random topology, resulting in a better diameter. These configurations show a reduction in network diameter by more than 100%.

On the contrary, the DGRO helps Perigee adopt the random ring topology, mainly because the ρ for Perigee is already very close to zero. The low value of ρ_{Perigee} results in significantly large diameters, especially as the number of nodes approaches 1000, proving to be highly unscalable. In such scenarios, DGRO helps the Perigee switches to a random ring and obtains a substantially low diameter of 20 – 30.

Hence, the single-heuristic approach can overlook other crucial aspects that contribute to an optimal network diameter, such as node distribution and link latencies, which a random ring might address by reducing the clustering of connections. Therefore, while the shortest ring topology may initially seem advantageous for minimizing diameter, it can lead to inefficiencies without considering the broader network context and the specific characteristics of the network’s topology. We next present an ablation study on how different combinations of shortest ring and random ring impact the diameter.

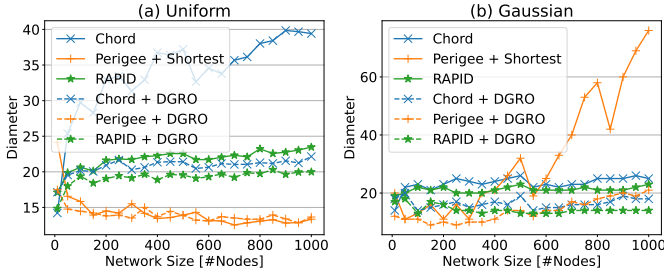


Figure 11: DGRO (dashed) reduces the diameter of CHORD (blue), Perigee (orange), and RAPID (green). Perigee is combined with a ring otherwise no connectivity guarantee.

2) *Ablation study on the number of random rings*: RAPID is structured around K random rings derived from K consistent hashing functions. In Figure 12, we modified up to M of these rings to the shortest heuristic, with M varying from 0 to K . The results show that for a uniform latency distribution, increasing M does not significantly improve the diameter; notably, when the network size approaches 1000, the diameter dramatically increases when all rings are shortest rings. Conversely, for a Gaussian distribution, the diameter decreases monotonically as M increases. Consequently, we developed DGRO to generalize across different latency distributions and network sizes, effectively adapting to the varying efficiencies observed under different configurations.

3) *DGRO*: Thanks to the capability of deep Q-learning to trade training time for solution quality, our DGRO model achieves a balance between random and shortest greedy approaches. As illustrated in Figure 13, the DGRO topology (red

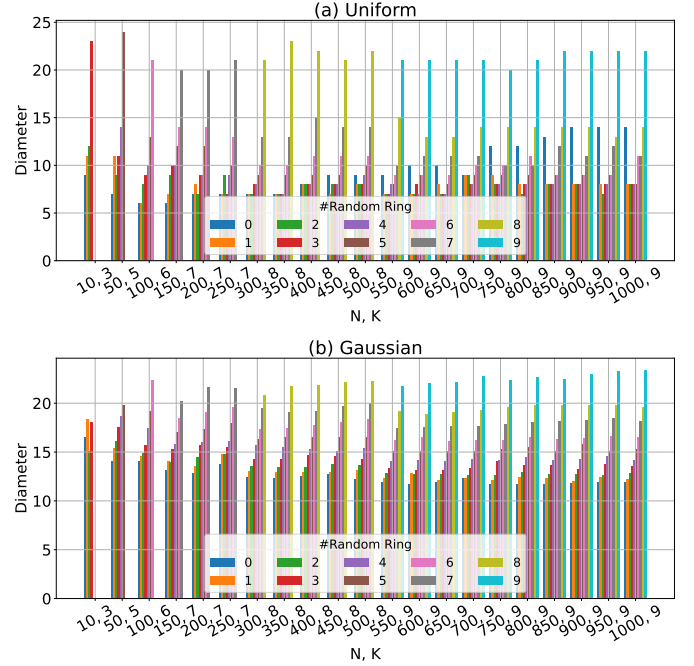


Figure 12: Benchmark how the number of DGRO rings impacts the diameter. Each color represents the number of random rings.

solid line) outperforms all six baselines in terms of diameter for both uniform and Gaussian distribution. Furthermore, DGRO demonstrates excellent scalability; as the network size approaches 1000, the diameter remains consistently stable, indicating the model’s robustness across larger network scales.

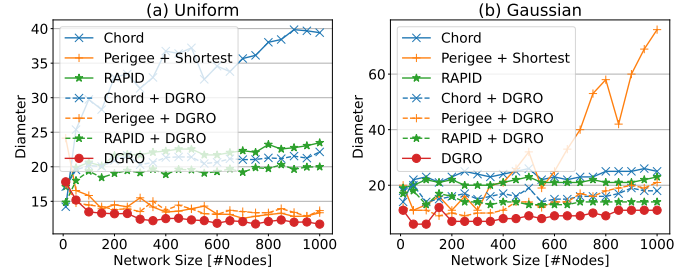


Figure 13: K-ring built by DGRO outperforms baselines.

4) *Parallel-DGRO*: In Figure 14, we evaluate the performance of DGRO when constructed in parallel. In this setup, a random ring is initially segmented into M partitions using a same stride, with each partition’s starting node determined by a consistent hash function. In Figure 14, the stride is set to $2^1 \sim 2^9$. Subsequently, these partitions concurrently reorder their internals using DGRO, while the construction within each partition is carried out sequentially. For both uniform and Gaussian distribution, the results show that even 8-partition DGRO is comparable to that of the original DGRO, illustrating the efficiency of parallel DGRO construction in optimizing network topology. Next, we present the result on the realistic dataset, FABRIC, and Bitnode.

D. Realistic Latency

1) *Single heuristic ring*: Figure 15 demonstrates how the ring selection can help reduce the diameter in two realistic datasets.

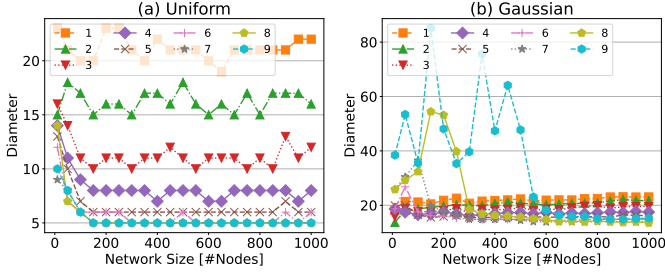


Figure 14: Parallel DGRO maintains the low diameter.

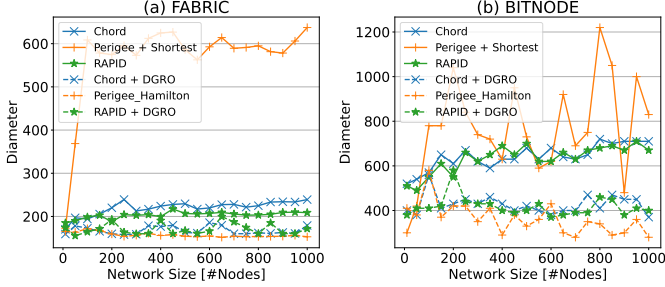


Figure 15: DGRO (dashed) reduces the diameter of CHORD (blue), Perigee (orange), and RAPID (green). Perigee is combined with a ring otherwise no connectivity guarantee.

For CHORD and RAPID, DGRO helps choose the shortest ring topology, which has lower diameter compared to a random ring. Conversely, in the case of Perigee, the random ring significantly outperforms the shortest ring.

2) *Ablation study on the number of random rings*: As shown in Figure 16, within the RAPID framework that employs a hybrid heuristic combining M random rings with $(K - M)$ shortest rings, there is no consistent value of M that consistently yields the best network diameter across different latency distributions and network sizes. This observation indicates that the optimal configuration of M varies depending on the specific characteristics of the network and the latency distribution, suggesting a need for a more adaptive approach to configuring these hybrid topologies.

3) *DGRO*: Figure 17 illustrated that DGRO consistently achieves a lower network diameter across a broad range of network sizes for both the FABRIC and Bitnode datasets compared to other methods. This performance demonstrates DGRO’s effectiveness in optimizing network connectivity and efficiency in diverse settings.

4) *Parallel DGRO*: Figure 18 tests the effectiveness of distributed construction on the FABRIC and Bitnode datasets. On the FABRIC dataset, using 2 to 32 partitions yields results similar to the original DGRO, demonstrating the model’s robustness across different partitioning schemes. On the Bitnode dataset, maintaining four partitions achieves a diameter comparable to a single-partition setup, indicating effective scalability and network management with minimal partitioning.

VIII. CONCLUSION

In this paper, we introduce **Diameter-Guided Ring Optimization (DGRO)**, which focuses on constructing rings with the smallest possible diameter, selecting the most effective

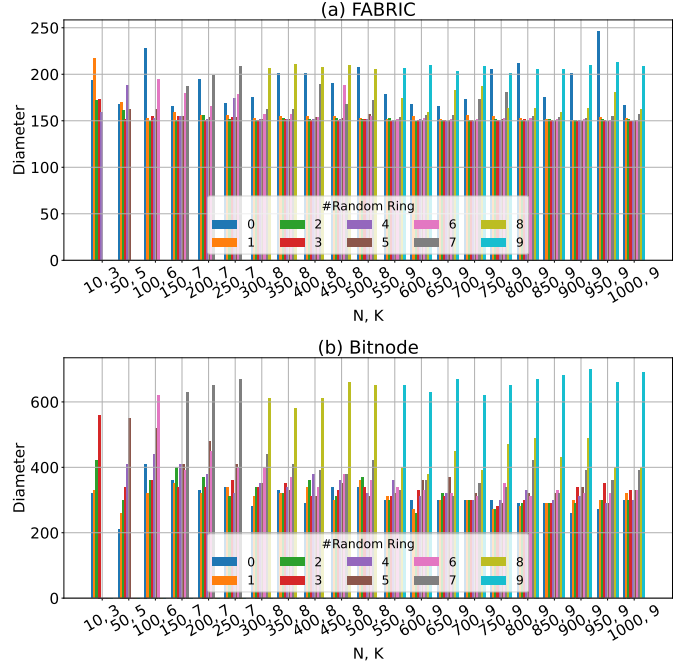


Figure 16: Benchmark how the number of DGRO rings impacts the diameter. Each color represents the number of random rings.

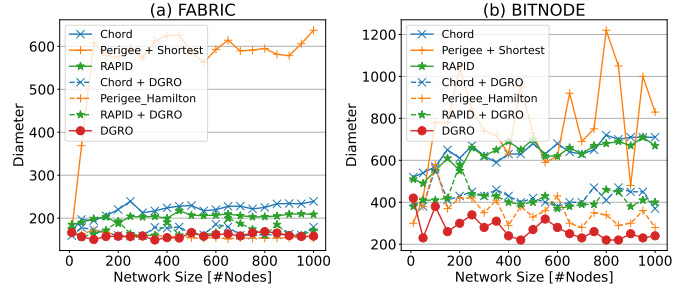


Figure 17: K-ring built by DGRO outperforms baselines.

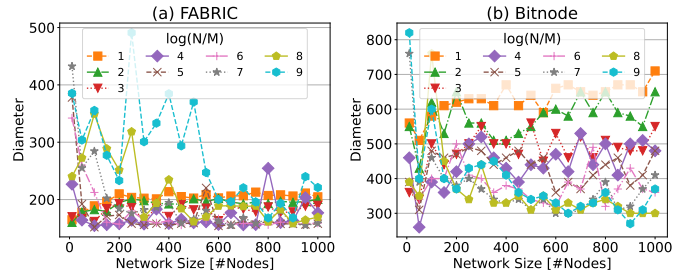


Figure 18: Parallel DGRO maintains the low diameter.

ring configurations, and implementing these configurations in parallel. We first explore an integration of deep Q-learning and graph embedding to optimize the ring topology. We next propose a ring selection strategy that assesses the current topology’s average latency against a global benchmark, facilitating integration into modern peer-to-peer protocols and substantially reducing network diameter. To further enhance scalability, we propose a parallel strategy that distributes the topology construction process into separate partitions simultaneously. In the future, we will integrate DGRO into a real system and evaluate its

performance in a real-world environment, such as Slurm [21]. Besides, we will explore the online update of DGRO.

REFERENCES

- [1] N. None, “Toward a seamless integration of computing, experimental, and observational science facilities: A blueprint to accelerate discovery,” USDOE Office of Science (SC), Washington, DC (United States). Advanced ..., Tech. Rep., 2021.
- [2] J. Liu *et al.*, “High-performance effective scientific error-bounded lossy compression with auto-tuned multi-component interpolation,” *Proceedings of the ACM on Management of Data*, vol. 2, no. 1, pp. 1–27, 2024.
- [3] Z. Jian *et al.*, “Cliz: Optimizing lossy compression for climate datasets with adaptive fine-tuned data prediction,” in *2024 IEEE International Parallel and Distributed Processing Symposium (IPDPS)*, IEEE, 2024, pp. 417–429.
- [4] J. Liu *et al.*, “Cusz-i: High-fidelity error-bounded lossy compression for scientific data on gpus,” *arXiv preprint arXiv:2312.05492*, 2023.
- [5] J. Huang *et al.*, “Exploring wavelet transform usages for error-bounded scientific data compression,” in *2023 IEEE International Conference on Big Data (BigData)*, IEEE, 2023, pp. 4233–4239.
- [6] B. Brown, “A vision for the ascr facilities enterprise,” in *Meeting of the Advanced Scientific Computing Advisory Committee*, 2021.
- [7] J. Ahrens *et al.*, “Envisioning science in 2050,” USDOE Office of Science (SC)(United States), Tech. Rep., 2022.
- [8] D. Bard *et al.*, “The lbl superfacility project report,” *arXiv preprint arXiv:2206.11992*, 2022.
- [9] L. A. Barroso and J. Clidaras, *The datacenter as a computer: An introduction to the design of warehouse-scale machines*. Springer Nature, 2022.
- [10] J. Dean and L. A. Barroso, “The tail at scale,” *Communications of the ACM*, vol. 56, no. 2, pp. 74–80, 2013.
- [11] P. Stelling, C. DeMatteis, I. Foster, C. Kesselman, C. Lee, and G. von Laszewski, “A fault detection service for wide area distributed computations,” *Cluster Computing*, vol. 2, pp. 117–128, 1999.
- [12] N. Losada, P. González, M. J. Martín, G. Bosilca, A. Bouteiller, and K. Teranishi, “Fault tolerance of mpi applications in exascale systems: The ulfm solution,” *Future Generation Computer Systems*, vol. 106, pp. 467–481, 2020.
- [13] D. A. Patterson, G. Gibson, and R. H. Katz, “A case for redundant arrays of inexpensive disks (raid),” in *Proceedings of the 1988 ACM SIGMOD international conference on Management of data*, 1988, pp. 109–116.
- [14] V. Sridharan and D. Liberty, “A study of dram failures in the field,” in *SC’12: Proceedings of the International Conference on High Performance Computing, Networking, Storage and Analysis*, IEEE, 2012, pp. 1–11.
- [15] K. Park, D.-H. Lee, Y. Woo, G. Lee, J.-H. Lee, and D.-H. Kim, “Reliability and performance enhancement technique for ssd array storage system using raid mechanism,” in *2009 9th International Symposium on Communications and Information Technology*, IEEE, 2009, pp. 140–145.
- [16] S. Wu *et al.*, “Anatomy of high-performance gemm with online fault tolerance on gpus,” in *Proceedings of the 37th International Conference on Supercomputing*, 2023, pp. 360–372.
- [17] S. Wu, Y. Zhai, J. Huang, Z. Jian, and Z. Chen, “Ft-gemm: A fault tolerant high performance gemm implementation on x86 cpus,” in *Proceedings of the 32nd International Symposium on High-Performance Parallel and Distributed Computing*, 2023, pp. 323–324.
- [18] S. Wu *et al.*, “Turbofft: A high-performance fast fourier transform with fault tolerance on gpu,” *arXiv preprint arXiv:2405.02520*, 2024.
- [19] S. Wu *et al.*, “Ft k-means: A high-performance k-means on gpu with fault tolerance,” *arXiv preprint arXiv:2408.01391*, 2024.
- [20] F. Cappello, G. Al, W. Gropp, S. Kale, B. Kramer, and M. Snir, “Toward exascale resilience: 2014 update,” *Supercomputing Frontiers and Innovations: an International Journal*, vol. 1, no. 1, pp. 5–28, 2014.
- [21] A. B. Yoo, M. A. Jette, and M. Grondona, “Slurm: Simple linux utility for resource management,” in *Workshop on job scheduling strategies for parallel processing*, Springer, 2003, pp. 44–60.
- [22] ETCD, *etcd*, <https://github.com/coreos/etcd>, 2014.
- [23] M. Burrows, “The chubby lock service for loosely-coupled distributed systems,” in *Proceedings of the 7th symposium on Operating systems design and implementation*, 2006, pp. 335–350.
- [24] A. ZooKeeper, *Apache zookeeper*, 2010.
- [25] NETFLIX, *netflix*, <https://github.com/Netflix/eureka>, 2014.

- [26] P. Kelley, "Eureka! why you shouldn't use zookeeper for service discovery," *Dosegljivo*: <https://tech.knewton.com/blog/2014/12/eureka-shouldnt-use-zookeeper-service-discovery>, 2014.
- [27] E. Hewitt, *Cassandra: the definitive guide*. "O'Reilly Media, Inc.", 2010.
- [28] TYPESAFE, *Akka*, <http://akka.io/>, 2009.
- [29] REDIS, *Redis*, <http://redis.io/>, 2009.
- [30] A. Newell, G. Kliot, I. Menache, A. Gopalan, S. Akiyama, and M. Silberstein, "Optimizing distributed actor systems for dynamic interactive services," in *Proceedings of the Eleventh European Conference on Computer Systems*, 2016, pp. 1–15.
- [31] L. Suresh, D. Malkhi, P. Gopalan, I. P. Carreiro, and Z. Lokhandwala, "Stable and consistent membership at scale with rapid," in *2018 USENIX Annual Technical Conference (USENIX ATC 18)*, 2018, pp. 387–400.
- [32] SCYLLA, *ScyllaDB*, <http://www.scylladb.com/>, 2013.
- [33] R. Van Renesse, Y. Minsky, and M. Hayden, "A gossip-style failure detection service," in *Middleware'98: IFIP International Conference on Distributed Systems Platforms and Open Distributed Processing*, Springer, 1998, pp. 55–70.
- [34] R. Van Renesse, K. P. Birman, and W. Vogels, "Astrolabe: A robust and scalable technology for distributed system monitoring, management, and data mining," *ACM transactions on computer systems (TOCS)*, vol. 21, no. 2, pp. 164–206, 2003.
- [35] A. Das, I. Gupta, and A. Motivala, "Swim: Scalable weakly-consistent infection-style process group membership protocol," in *Proceedings International Conference on Dependable Systems and Networks*, IEEE, 2002, pp. 303–312.
- [36] C. McCaffrey, *Building scalable stateful services*, <https://speakerdeck.com/caitiem20/building-scalable-stateful-services>, Accessed: 2024-10-10, 2015.
- [37] L. Benini and G. De Micheli, "Networks on chips: A new soc paradigm," *computer*, vol. 35, no. 1, pp. 70–78, 2002.
- [38] N. Laoutaris, L. J. Poplawski, R. Rajaraman, R. Sundaram, and S.-H. Teng, "Bounded budget connection (bbc) games or how to make friends and influence people, on a budget," in *Proceedings of the twenty-seventh ACM symposium on Principles of distributed computing*, 2008, pp. 165–174.
- [39] E. D. Demaine and M. Zadimoghaddam, "Minimizing the diameter of a network using shortcut edges," in *Scandinavian Workshop on Algorithm Theory*, Springer, 2010, pp. 420–431.
- [40] A. Meyerson and B. Tagiku, "Minimizing average shortest path distances via shortcut edge addition," in *International Workshop on Approximation Algorithms for Combinatorial Optimization*, Springer, 2009, pp. 272–285.
- [41] R. B. Tan, E. J. Van Leeuwen, and J. Van Leeuwen, "Shortcutting directed and undirected networks with a degree constraint," *Discrete Applied Mathematics*, vol. 220, pp. 91–117, 2017.
- [42] V. Chepoi and Y. Vaxes, "Augmenting trees to meet biconnectivity and diameter constraints," *Algorithmica*, vol. 33, pp. 243–262, 2002.
- [43] C.-L. Li, S. T. McCormick, and D. Simchi-Levi, "On the minimum-cardinality-bounded-diameter and the bounded-cardinality-minimum-diameter edge addition problems," *Operations Research Letters*, vol. 11, no. 5, pp. 303–308, 1992.
- [44] F. R. Chung and M. R. Garey, "Diameter bounds for altered graphs," *Journal of graph theory*, vol. 8, no. 4, pp. 511–534, 1984.
- [45] Bokhari and Raza, "Reducing the diameters of computer networks," *IEEE transactions on computers*, vol. 100, no. 8, pp. 757–761, 1986.
- [46] K. Garimella, G. De Francisci Morales, A. Gionis, and M. Mathioudakis, "Reducing controversy by connecting opposing views," in *Proceedings of the tenth ACM international conference on web search and data mining*, 2017, pp. 81–90.
- [47] S. Haddadan, C. Menghini, M. Riondato, and E. Upfal, "Republik: Reducing polarized bubble radius with link insertions," in *Proceedings of the 14th ACM International Conference on Web Search and Data Mining*, 2021, pp. 139–147.
- [48] R. Interian, J. R. Moreno, and C. C. Ribeiro, "Polarization reduction by minimum-cardinality edge additions: Complexity and integer programming approaches," *International Transactions in Operational Research*, vol. 28, no. 3, pp. 1242–1264, 2021.
- [49] O. Vinyals, M. Fortunato, and N. Jaitly, "Pointer networks," *Advances in neural information processing systems*, vol. 28, 2015.
- [50] I. Bello, H. Pham, Q. V. Le, M. Norouzi, and S. Bengio, "Neural combinatorial optimization with reinforcement learning," *arXiv preprint arXiv:1611.09940*, 2016.
- [51] A. Graves *et al.*, "Hybrid computing using a neural network with dynamic external memory," *Nature*, vol. 538, no. 7626, pp. 471–476, 2016.
- [52] H. Dai, E. Khalil, Y. Zhang, B. Dilkina, and L. Song, "Learning Combinatorial Optimization Algorithms over Graphs," *Advances in neural information processing systems*, vol. 30, 2017.
- [53] J. Johnston, X.-Y. Liu, S. Wu, and X. Wang, "A curriculum learning approach to optimization with application to downlink beamforming," *IEEE Transactions on Signal Processing*, 2023.
- [54] X.-Y. Liu, Z. Li, S. Wu, and X. Wang, "Stationary deep reinforcement learning with quantum k-spin hamiltonian regularization," in *ICLR 2023 Workshop on Physics for Machine Learning*, 2023.
- [55] J. Johnston, X.-Y. Liu, S. Wu, and X. Wang, "Downlink beamforming optimization via deep learning," in *2023 59th Annual Allerton Conference on Communication, Control, and Computing (Allerton)*, IEEE, 2023, pp. 1–5.
- [56] F. Adriaens and A. Gionis, "Diameter minimization by shortcutting with degree constraints," in *2022 IEEE International Conference on Data Mining (ICDM)*, IEEE, 2022, pp. 843–848.
- [57] I. Stoica, R. Morris, D. Karger, M. F. Kaashoek, and H. Balakrishnan, "Chord: A scalable peer-to-peer lookup service for internet applications," *ACM SIGCOMM computer communication review*, vol. 31, no. 4, pp. 149–160, 2001.
- [58] Y. Mao, S. Deb, S. B. Venkatakrishnan, S. Kannan, and K. Srinivasan, "Perigee: Efficient Peer-to-Peer Network Design for Blockchains," in *Proceedings of the 39th Symposium on Principles of Distributed Computing*, 2020, pp. 428–437.